Article:

Chapman, S orcid.org/0000-0002-3141-8616, Thatcher, M, Salazar, A et al. (2 more authors) (2019) The impact of climate change and urban growth on urban climate and heat stress in a subtropical city. International Journal of Climatology, 39 (6). pp. 3013-3030. ISSN 0899-8418

https://doi.org/10.1002/joc.5998

The impact of climate change and urban growth on urban climate and heat stress in a subtropical city

The impact of climate change and urban growth on heat stress

Sarah Chapman[1, *], Marcus Thatcher[2], Alvaro Salazar[1, 3, 4], James E.M. Watson[1, 5] and Clive A. McAlpine[1]

1. The University of Queensland, School of Earth and Environmental Sciences, St Lucia, QLD 4072, Australia
2. CSIRO Marine and Atmospheric Research, Aspendale, VIC 3195, Australia
3. Departamento de Biología, Facultad de Ciencias, Universidad de La Serena, Casilla 554, La Serena, Chile
4. Instituto de Ecología y Biodiversidad (IEB)
5. Global Conservation Program, Wildlife Conservation Society, Bronx, NY 10460, USA

* Corresponding author contact information: s.chapman@uq.edu.au, Tel.: +61 3346 1652

Funding Information:

SC was supported by an Australian Postgraduate Award. This project was supported by Australian Research Council Discovery Project DP160102107.

Abstract

Urban residents face increasing risk of heat stress due to the combined impact of climate change and intensification of the urban heat island (UHI) associated with urban growth. Considering the combined effect of urban growth and climate change is vital to understanding how temperatures in urban areas will change in the future. This study investigated the impact of urban growth and climate change on the UHI and heat stress in a sub-tropical city (Brisbane, Australia) in the present day (1991-2000) and medium term (2041-2050; RCP8.5) during summer. A Control and Urban Growth scenario were used to compare the temperature increase from climate change alone with the temperature increase from climate change and urban growth. Average and minimum temperatures increased more with climate change and urban growth combined than with climate change alone, indicating that if urban growth is ignored, future urban temperatures could be under-estimated. Under climate change alone, rural temperatures increased more than urban temperatures, decreasing the effect of the UHI by 0.4°C at night and increasing the urban cool island by 0.8°C during the day. With climate change, the number of hot days and nights doubled in urban and rural areas in 2041-2050 as compared to 1991-2000. The number of hot nights was higher in urban areas and with urban growth. Dangerous heat stress, defined as Apparent Temperature above

This article has been accepted for publication and undergone full peer review but has not been through the copyediting, typesetting, pagination and proofreading process, which may lead to differences between this version and the Version of Record. Please cite this article as doi: 10.1002/joc.5998

40°C, increased with climate change, and occurred on average 1-2 days every summer during 2041-2050, even in shaded conditions. There was higher temperature increases with urban growth and climate change than with climate change alone, indicating that reducing the effect of the UHI is vital to ensuring urban growth does not increase the heat stress risks that urban residents will face in the future.

Keywords: urban heat island, climate change, heat stress, sub-tropical

1. Introduction

Extreme heat is the leading weather-related cause of death in highly urbanised countries such as the USA and Australia (Coates et al., 2014; Environmental Protection Agency, 2016). During heat waves, the death toll can rise to the thousands, as seen in Europe in 2003 and 2010 (Barriopedro et al., 2011; Robine et al., 2008), France in 2006 (Fouillet et al., 2008) and Asia in 2015 (World Meteorological Organization, 2016). Urban residents are particularly vulnerable to heat stress due to the 'urban heat island' (UHI), whereby cities are warmer than the surrounding countryside, mainly at night (Heaviside et al., 2017; Medina-Ramón & Schwartz, 2007). During heatwaves, urban residents are exposed to greater risk of heat stress and higher mortality than rural residents due to the UHI (Clarke, 1972; Hayhoe et al., 2010). Given over half of the world's population lives in cities (United Nations, 2014) understanding heat stress is essential for allowing urban populations to better adapt to almost certain higher future temperatures (Fouillet et al., 2008).

The UHI occurs due to urban modification of land cover and can result in increases in urban temperatures by on average 2°C. Urban areas can also be cooler than rural areas, termed an "urban cool island", and can occur in the early morning due to urban areas warming up more slowly than rural areas in response to solar radiation, and in arid areas if cities have extensive irrigation. Under weather conditions of low wind speed and cloud cover, the increase in temperatures in urban areas can be as high as 10°C (Arnfield, 2003; Chang et al., 2007; Gedzelman et al., 2003; Sharifi & Lehmann, 2014; Wilby, 2008). The UHI occurs in the surface, sub-surface, canopy layer, which is the air above the ground and below rooftops, and the boundary layer (Oke, 1995; Yow, 2007). The canopy layer is the most relevant for human health as most activity occurs in this layer and is the focus of this study (Yow, 2007). The UHI is more frequent and pronounced during the night, when adjacent rural residents would experience relief from the heat (Clarke, 1972). The main factors influencing the formation of the UHI are associated with urban form, and include building height, height/width ratio, green space, anthropogenic heat release and weather (Arnfield, 2003; Oke, 1982). Building height and height/width ratio both act to reduce the sky-view factor and the amount of outgoing radiation as compared to rural areas (Chun & Guldmann, 2014; Unger, 2009). Tall buildings can also have a shading effect during the day, and reduce incoming solar radiation (Chun & Guldmann, 2014). The amount of green space is a key contributor to the UHI. Less greenspace reduces the capacity for evapotranspiration, with more energy partitioned into sensible rather than latent heat (Oke, 1982; Taha, 1997). As building density increases and green space decreases, the intensity of the UHI will increase (Arnfield, 2003; Oke, 1973; Parker, 2010), thereby increasing the risk of heat stress to urban residents.

Considering the combined impacts of urbanization and climate change on future urban temperatures is vital, as they both have large impacts on future heat stress, particularly in low-income countries with little capacity to adapt to rising temperatures (Althor et al., 2016; Argüeso et al., 2015; IPCC, 2014). Neglecting to consider the interaction effects between urban growth and climate change can result in the under-estimation of the magnitude of future urban heat stress (Chapman et al., 2017). Urban areas may also respond differently to climate change than rural areas (McCarthy et al., 2010; Oleson, 2012).

The main mechanisms by which urban and rural areas may respond differently to climate change are weather (wind speed and cloud), evapotranspiration and anthropogenic heat release (Hoffmann et al., 2012; McCarthy et al., 2010; Oleson, 2012). The most intense UHI effect occurs under conditions of low wind speed and low cloud cover (Bonan, 2008; Oke, 1982), thus any changes to winds and clouds from climate change could alter the frequency of high-intensity UHIs (Hoffmann et al., 2012). Urban and rural differences in evapotranspiration are also a key contributor to the UHI. If soils dry out due to climate change, rural evapotranspiration will decrease, while urban areas, with less bare soil, may be less affected and experience less of a reduction in evapotranspiration (Oleson, 2012). This could lead to rural areas warming more than urban areas with climate change due to a bigger reduction in evapotranspiration and latent heat flux (Oleson, 2012). Anthropogenic heat release is the heat released from human activities, such as heating and cooling of buildings, vehicle usage, and human metabolism (Sailor & Lu, 2004). Increases in the amount of air-conditioning used in buildings due to rising temperatures with climate change would increase anthropogenic heat release in cities, further increasing the UHI, and reductions in the amount of heating required in high-latitude cities could decrease anthropogenic heat release and the UHI (Oleson, 2012). The interaction between climate change the UHI is a key research gap, hampering our understanding of future urban temperatures (Chapman et al., 2017).

In this study, we examined the impact of urban growth and climate change on the climate and heat-stress of Brisbane, a sub-tropical city in eastern Australia, in 2041-2050. We conducted two high-resolution modelling experiments of the impact of climate change alone, and climate change combined with a scenario of urban densification. The first scenario used the present-day land cover with RCP8.5, while the second scenario used a medium density urban growth scenario with RCP8.5 to examine the combined impact of urban growth and climate change on the urban heat island during summer from 2041-2050.

2. Methods

2.1. Study area

Brisbane is the third largest city in Australia, with a population of 1.9 million people (Figure 1). It has a sub-tropical climate, with summer-dominant rainfall (Bureau of Meteorology, 2017). Mean monthly temperatures range from 21.7 to 28.5°C (Bureau of Meteorology, 2017). Between 1999 and 2018, there were on average 70 days a year when maximum temperature exceeded 30°C, as measured at the Brisbane City station, station ID 040913 (Bureau of Meteorology, 2017). By 2050, Brisbane's population is expected to increase to 3.5-4.7 million people (Australian Bureau of Statistics, 2013). Most of the urban development associated with this growth will be via densification rather than geographic expansion of the urban area (Brisbane City Council, 2014).

{Fig. 1}

2.2. Model configuration

We used CCAM (Conformal Cubic Atmospheric Model), developed by the CSIRO, to run high-resolution (1 km grid cell) climate simulations over Brisbane City. CCAM uses a tile approach, with a grid box composed of a combination of vegetation and urban tiles. Vegetation is modelled using the CABLE land surface scheme and urban areas using ATEB (Australian Town Energy Budget). ATEB is an urban canopy model which allows CCAM to simulate the urban climate (Thatcher & Hurley, 2012). The model physics schemes are listed in Table 1.

ATEB is based on the Town Energy Budget model and has been updated to reflect the Australian context; idealized air-conditioners have been parameterized, the urban vegetation component has been altered to better reflect the vegetation in Australian suburbs and the model now includes consideration of two canyon walls facing easterly and westerly directions (Masson, 2000; Thatcher & Hurley, 2012). Vegetation in urban areas is modelled using a big-leaf model and is primarily modelled as 1 m shrubs (Thatcher & Hurley, 2012).

ATEB has previously been used to model urban climates in Australian cities (Chen et al., 2015; Chen et al., 2014; Luhar et al., 2014; Ren et al., 2014).

{Tab. 1}

For our experiments, the model was first run with a quasi-uniform global resolution of 100 km using a C96 grid. The model was then run in stretched grid mode and downscaled to 60km, 8km and then 1 km resolution over the following regions: 0°-60°S, 105°-165°E, 25.5°-29.5°S, 151°-155°E and 27.2°-27.8°S, 152.7°-153.5°E (see Figure 1). We used a global stretched C48 grid and extracted data from the high-resolution area (1 km domain), which used 48 × 48 gridpoints. A total of 27 vertical model levels were used, ranging from 20 m-35 km, with 10 levels in the first 1000 m. The orography data used in CCAM has a 250 m resolution over Australia and was provided by Geoscience Australia.

CCAM was forced using bias corrected sea-surface temperatures from ACCESS 1.0, a global climate model developed by the CSIRO and the Australian Bureau of Meteorology (Bi et al., 2013). The bias correction method is described in Hoffmann, Katzfey, et al. (2016), and performed on the inputs to CCAM. This method results in improvements in mean and interannual variability in climate variables, as compared to non-corrected SSTs (Hoffmann, Katzfey, et al., 2016).

2.3. Experimental design

Two experiments (Table 2) were conducted to evaluate the effect of urban growth and climate change on urban climate.

{Tab. 2}

The 100 km run of CCAM was simulated continuously from 1990-2050. The 60 and 8 km runs ran in the two time periods of interest (1990-2000 and 2040-2050). The 1 km simulation was run for Nov-Feb, with November acting as a month of spin up prior to the austral summer. The 8 km run, which ran continuously through the periods of interest, provided the initial conditions for the 1 km run.

The land cover maps were based on MODIS 2001 land cover data, with the IGBP classification scheme (Global Land Cover Facility, 2018). In addition, two new urban categories were added: urban-high density and urban-medium density. The parameters for each urban category in ATEB were based on measurements from Melbourne, Australia, and are shown in Table 3 (Coutts et al., 2007). The only change from the MODIS land cover for the Control scenario was the addition of the CBD (central business district) as a high-density area.

For the Urban Growth scenario, land cover within the inner half of the urban area was changed from low to medium density. This resulted in an increase in building height of 2 m, a reduction in the amount of green space by 11%, and an increase in the height/width ratio of 0.2. Green space refers to in-canyon vegetation and is modelled in ATEB using a big-leaf model. This urban growth scenario is broadly consistent with Brisbane's future planned growth, the majority of which (88% of the planned additional dwellings) will be achieved by increasing density in inner city areas, rather than expansion of the urban area (Brisbane City Council, 2014).

{Tab. 3}

The maps of land cover for the Control and Urban Growth scenarios are shown in Figure 2.

{Fig. 2}

The scenarios were compared using minimum, maximum and average temperature, the energy budget, the UHI, the number of hot days and nights, and heat stress indices. In these comparisons, rural land areas within the same elevation range of urban areas were used, to minimize the effect of elevation on climate.

2.4. UHI Calculation

The ability of CCAM, in combination with ATEB, to reproduce the Brisbane UHI has previously been validated (Chapman et al., 2018). For this study, the UHI was calculated using an urban and rural point, which are shown in Figure 2. Weather station locations were not used given that for the period, 1991-2000, there are no weather stations operating continuously (> 5 years, < 25% missing data) in rural and inner-city locations for the UHI calculation. The UHI was calculated as $Temp_{urban} - Temp_{rural}$ for the present day and the mid-term, and for the Control and Urban Growth scenarios.

The rural point was chosen to minimize the differences in elevation between it and the urban point, while also maintaining distance from urban areas, and at a similar distance to the ocean as the urban point.

2.5. Number of hot days and nights

Hot days were defined as days with maximum temperature above the 95th percentile of maximum temperature for 1991-2000 Control rural areas. Hot nights are defined the same way, using minimum temperature. The threshold temperature for hot days was 40°C and 24°C for hot nights.

The difference in the number of hot days and nights between scenarios was statistically tested using the Kruskal-Wallis test. The data was averaged over the 10-year period, resulting in one value for each grid cell, and then grouped into rural, low density and medium density areas. The CBD was not included in statistical tests as it covers only a small area in CCAM and so does not have a sufficient sample size.

Only rural areas within the same elevation range (1-159 m) similar to urban areas were included, to minimize the influence of elevation on temperature. A 25 m resolution digital elevation model for South-East Queensland was used to determine the elevation range of urban areas in Brisbane (Department of Natural Resources, 2013). Water bodies were not included in these calculations.

2.6. Heat stress calculation

Heat stress occurs when core body temperature rises above 37 ^{0}C (Epstein & Moran, 2006; Sherwood et al., 2010; Taylor, 2006). The human body maintains its temperature by exchanging heat with the environment (Epstein & Moran, 2006). The rate of exchange is governed by heat produced by the body, heat gained from the environment and sweat evaporation (Epstein & Moran, 2006). Heat stress is not just affected by temperature, but by factors relating to evaporation, such as air movement and humidity, as well as type of activity and clothing (Budd, 2008; Buzan et al., 2015; Epstein & Moran, 2006). Numerous indexes (>40) have been developed to measure heat stress (Epstein & Moran, 2006). No single index is superior in all situations (Brake & Bates, 2002; Kim et al., 2011; Morabito et al., 2014). An index that is widely used is the wet-bulb globe temperature (WBGT) (Budd, 2008; d'Ambrosio Alfano et al., 2014; Ooka et al., 2010; Taylor, 2006). Apparent Temperature (AT) is also widely used, including by the Australian Bureau of Meteorology (2010), and the shade version has been found to be related to heat-stress mortality in cities near the coast (Morabito et al., 2014).

Three direct heat stress indices were calculated: WBGT, AT for sun (AT_{sun}), and shade (AT_{shade}). For all the heat stress calculations, daily average temperature was used. For outdoor conditions, the WBGT is calculated as follows (Epstein & Moran, 2006):

$$WBGT = 0.7T_w + 0.2T_g + 0.1T_d \quad (1)$$

…where T_w = wet-bulb temperature, T_g = globe temperature and T_d = dry bulb temperature. T_g was calculated using the following formula (Hajizadeh et al., 2017):

$$T_g = 0.01498S + 1.184T_d - 0.0789RH - 2.739 \quad (2)$$

Accepted Article

…where S = solar radiation (w/m^2) and RH = relative humidity (%).

T_w was calculated using the Davies-Jones (2008) equation, as calculated using the HumanIndexMod developed by Buzan et al. (2015).

The shade version of AT (AT_{shade}) was calculated using the following equation as implemented in the HumanIndexMod (Buzan et al., 2015):

$$AT_{shade} = T_d + 0.33e - 0.7U_{10} - 4.00 \quad (3)$$

The equation for AT_{sun} is as follows (Steadman, 1984):

$$AT_{sun} = 4.5. + 10.2T_d - 1.00U_{10} + 0.28e - 5.8D + 0.0054\,(Q_D + Q_d) \quad (4)$$

…where e = water vapour pressure in hPa, D = fraction of solar radiation that is direct, Q_D = direct solar radiation and Q_d = diffuse solar radiation. D estimated based on daytime (6am-6pm) values from CCAM, which is calculated by the GFDL-CM2.1 radiation code (Schwarzkopf & Fels, 1991; Schwarzkopf & Ramaswamy, 1999)

Only rural areas within the same elevation range as urban areas were used to calculate rural heat stress, to minimize the influence of elevation on temperature. The calculated indices were then compared to threshold values which define levels of danger and activity. WBGT was compared to Sports Medicine Australia guidelines (2007), and AT was compared to USA National Weather Service Heat Index Guidelines (2018). Heat Index guidelines are used for AT as the Heat Index is a simplified version of AT.

3. Model validation

The ability of the model to reproduce summer air temperature was evaluated by comparing the Control average, minimum and maximum temperature, 10 m wind speed and relative humidity with observational data from seven Bureau of Meteorology weather stations (See Table 4 and Figure 2). Average temperature was calculated based on three-hourly temperature data from the Bureau of Meteorology, while minimum and maximum temperature were calculated based on daily minimum and maximum temperature data. Samford and Logan were excluded from the calculation of average temperature bias as data was only available at 9am for Samford, and 9am and 3pm for Logan, which would give a misleading estimate of average temperature. For Annerley, observational average temperature was only compared with model data from February 1992 onwards, as prior to that hourly data was only available at 9am and 3pm.

For the model validation only, the output temperature data from CCAM was corrected to account for the difference in elevation between CCAM and the weather stations. This correction was -6.5°C per km. Samford and Redcliffe had the biggest elevation difference between the model and weather stations at 13 and 13.2 m respectively. All other stations were within 7.5 m of the model elevation.

During the present-day period (December 1990-February 2000) only two of the seven weather stations were open the entire time. Missing data was also an issue for the remaining stations. Only stations that were missing less than 25% of their data during the time they were open and were open for at least 5 years between Dec 1990 and Feb 2000, were included in the model validation. The years open and amount of missing data are shown in Table S1.

{Tab. 4}

Based on average monthly data, the average summer temperature of the model was 0.8°C warmer than observations. Minimum temperature was 0.9°C cooler than observations and maximum temperature was 2.1°C warmer. Logan had the largest bias, and the model minimum temperature was 5.5°C too cool here. The elevation of the Logan station is similar to the other stations; however, it is surrounded by hilly topography. This may not be adequately captured by the 1 km resolution of the model and may be contributing to the higher bias at this station.

4. Results

4.1. Climate and urban growth impact on temperature

Temperature changes due to climate change and urbanisation were examined by comparing Control and Urban Growth 2041-2050 temperatures with the Control 1991-2000 temperatures (Table 5). Average summer air temperatures for Control 2041-2050 were 2.5°C higher compared to the 1991-2000 temperatures. Maximum temperature increased more than average temperature, by an average of 2.8°C. The temperature increases in the Urban Growth scenario were higher than in the Control scenario for average and minimum temperature, by up to 0.4°C in the CBD. For both scenarios, maximum temperature in rural areas increased more than urban temperatures by up to 1°C in 2041-2050. Increases in average, minimum and maximum temperature were statistically significant at the 95% confidence interval across the entire study area, as evaluated using a modified t-test that accounts for serial correlation in spatial climatological data (Zwiers & Storch, 1995).

{Tab. 5}

4.2. Urban heat island comparison

The average hourly variation in the summer UHI during the present day, 1991-2000, and medium term, 2041-2050, for the Control and Urban Growth scenario are shown in Figure 3. The UHI was calculated as the temperature difference between the urban and a rural point, as shown in Figure 2. The average summer UHI from 1991-2000 was 0.8°C for the Control and 0.9°C for the Urban Growth scenario. By 2041-2050, this decreased by 0.6°C for the Control and the Urban Growth scenario. For both scenarios, the change in the UHI was higher during the day than during the night. The daytime urban cool island (when urban areas are cooler than rural areas) increased by -0.8°C, while at night, the urban heat island decreased by -0.4°C. The maximum daytime cool island intensified in the mid-term by 1.1°C for the

Control and 1.2°C for the Urban Growth scenario. The maximum value of the nocturnal UHI decreased from 2.8°C to 2.4°C for the Control, and from 3.1°C to 2.8°C for the Urban Growth scenario.

The early morning (4-7am) UHI does not change much with climate change. During these hours, the intensity of the UHI is driven by the warming in response to sunrise. Before sunrise, urban areas are warmer than rural areas. At sunrise, rural areas warm up quickly, more so than urban areas, (Figure S1), reducing the intensity of the UHI, until an urban cool island develops.

{Fig. 3}

The number of extreme UHIs also decreased. During 1991-2000, there were on average 20 days per summer when the UHI was greater than 5°C for the Control, and 27 days for the Urban Growth scenario. During 2041-2050, the number of days with a UHI greater than 5°C nearly halved for the Urban Growth scenario to 15 days, and was halved for the Control scenario, down to 9 days. In the present-day climate, UHI events exceeding 7°C occurred on average 3 days per summer in the Control scenario and 4 days per summer in the Urban Growth scenario. In 2041-2050, these events occurred on average only once per summer for the Control, and twice per summer for the Urban Growth scenario.

4.3. Energy Budget

The reduction in the UHI reflects a stronger warming of rural areas compared to urban areas (Figure 4). This is most apparent in the Urban Growth scenario and for maximum temperature. The urban areas of Brisbane are closer to the ocean, which may explain some of the smaller increase in urban temperatures as compared to rural temperatures.

{Fig. 4}

The increasing rural temperatures are also associated with changes in the latent heat flux, which decreased more in rural areas than in urban areas (Figure 5). The reduction in latent heat flux reflects a drying trend under RCP8.5; rainfall decreases, as does soil moisture (see Figures S2-S3) and relative humidity. In addition, incoming longwave and solar radiation increase (see Figure S4). Longwave radiation increases due to higher upper air temperatures, while solar radiation increased due to a small reduction in cloud cover during this period (see Figure S2). With increasing energy and reduced water, there is less potential for cooling with evapotranspiration, which contributes to higher temperatures, particularly in rural areas which have a higher latent heat flux than urban areas and rely more on cooling by evapotranspiration than urban areas.

{Fig. 5}

The increased drying trend is exacerbated in the Urban Growth scenario, which experienced larger reductions in latent heat flux than the Control scenario, particularly in rural areas close to the city. The drier urban air also may be affecting the nearby rural areas in this scenario. The increased drying trend and higher warming in rural areas acts to reduce the difference in latent heat flux and temperature between urban and rural areas, and thus reduces the UHI.

4.4. Hot days and nights

Under RCP8.5, the number of hot days (max temp > 40°C) and nights (min temp > 24°C) increased for both the Control and Urban Growth scenario. Hot days were defined as days with maximum temperature above the 95th percentile of maximum temperature in rural areas for 1991-2000 Control. Hot nights were defined same way, using minimum temperature. The increase in hot days and nights with climate change was statistically significant at $p < 0.05$ for all scenarios and areas.

The Urban Growth scenario experienced more hot nights at each urban location than the Control scenario. The biggest difference in the number of hot nights between the two scenarios was in areas that changed from low to medium density ("Medium Density" in Figure 6), and the CBD (Figure 6, panel d2), where land cover did not change between the two scenarios. This difference in the number of hot nights between the Urban Growth and Control scenario was statistically significant at $p < 0.05$ in Medium Density areas in both the present day and midterm and was significant in low density and rural areas in the present day at $p < 0.1$. The Control scenario had more hot days than the Urban Growth scenario in the CBD and the Medium Density urban areas, though the difference was smaller than for hot nights and was only statistically significant in the present day, not the midterm, and only in medium density and rural areas. The CBD covers a small spatial area in CCAM and was not included in the statistical tests. This also leads to the small error bars in Figure 6.

For the Control scenario, the average number of hot days and nights doubled for each area from the present day to the medium term (Figure 6). In rural areas, the average number of hot nights in summer more than tripled, increasing from three to 17 nights per summer for both scenarios. For the Urban Growth scenario, the average number of hot nights tripled in Medium Density areas, increasing from 15 to 48 nights. At the CBD, the average number of hot nights per summer increased from 19 to 55 for the Urban Growth scenario, and 14 to 47 for the Control scenario.

{Fig. 6}

Specific locations were examined to identify the duration of hot events. The CBD and rural point used in the UHI calculation were chosen to represent CBD and rural areas respectively and the Archerfield weather station was used to represent Medium Density areas.

Consecutive hot day events, with maximum temperatures above 40°C for three days or longer, lasted for longer for both scenarios in the medium term than in the present day. Over the ten-year period 2041-2050, hot day events occurred five times for the Control and six times for the Urban Growth scenario in rural areas. In urban areas in 2041 - 2050, hot day events occurred three times for the Control and twice for the Urban Growth scenario. This is an increase from 1991-2000, when hot day events of three days or more occurred only once for the Control and twice for the Urban Growth scenario in rural areas and did not occur in urban areas.

Consecutive hot night events lasted for longer at urban locations in the Urban Growth scenario than in the Control scenario. In 2041-2050, on average, hot night events lasting longer than three nights occurred three times per summer for the Control and Urban Growth scenario at Archerfield. At the CBD, hot night events lasting longer than three nights occurred four times per summer in the Control, and six times per summer in the Urban Growth scenario. Long events (>= 14 consecutive nights) occurred only during the medium term, and not in the present day. Over the 2041-2050 period, events with hot nights that lasted for 14 days or longer occurred 3 times for the Control and 6 times for the Urban Growth scenario in urban areas. The longest duration events occurred in the CBD in the Urban Growth scenario.

4.5. Heat stress indices

Heat stress was calculated using WBGT and AT for sun and shade. These indices were then compared to threshold values that provide guidelines for level of activity. AT_{shade} reflects the heat stress for people working and doing activity outdoors in the shade, while AT_{sun} reflects the heat stress people would face if they were active in direct sun.

We also compared the threshold values of WBGT and AT, calculated with daily average temperature. Thresholds for WBGT are based on Sports Medicine Australia guidelines. For ‘Moderate’ WBGT (WBGT between 21-25), Sports Medicine Australia recommends taking more breaks during activity, for ‘High’ (WBGT between 26-29) they recommend limiting the intensity and duration of exercise (Sports Medicine Australia, 2007). AT guidelines are based on the USA National Weather Service Heat Index Guidelines (2018). ‘Moderate’ (AT between 36.7-32.1) indicates fatigue possible with prolonged exposure or physical activity, ‘High’ (AT between 32.2-40.5) indicates heat stroke, cramps or exhaustion possible with prolonged exposure or physical activity, and ‘Danger’(AT > 40.6) indicates heat cramps and exhaustion likely, and heat stroke possible with prolonged exposure or physical activity (National Weather Service, 2018). Using average temperature, there is minimal difference in the heat stress indices between low, medium density areas and the CBD urban area. As with temperature, the average UHI as calculated with heat stress also decreases slightly from the present day to the midterm by 0.3-0.5 for all indices, while absolute heat stress increases. The average number of days per summer with high and dangerous heat stress risk increased with RCP8.5 (Figure 7). With RCP8.5, dangerous heat stress occurs 1-2 days per summer (AT_{shade}) during 2041-2050, and 6-7 days per summer when in the sun (AT_{sun}). With RCP8.5, high heat stress risk, measured with AT_{sun}, occurs over 60 days per summer for both rural and urban areas and for both scenarios. For WBGT and AT_{shade}, high heat stress increases by more than 4 times the present-day value and occurs 23 days per summer in rural areas and 19-22 days per summer in urban areas using WBGT and using AT_{shade} occurs 18 days per summer in rural areas and 12-15 days per summer in urban areas. Using average temperature to calculate these indices, there is minimal difference in the number of days above thresholds for urban and rural areas. For AT_{sun}, urban growth leads to 2-3 extra days per summer with high heat stress in urban areas where land cover changed.

{Fig. 7}

5. Discussion

5.1. Overview

In this study, we used a high-resolution atmospheric model coupled with an urban canopy model to investigate the impact of climate change and urban growth on the UHI and heat stress of a sub-tropical city in Australia. Using a scenario of inner-city urban growth in combination with the RCP 8.5 climate scenario, we demonstrate that climate change increases temperature everywhere. When climate change and urbanisation are considered together, the temperature increases are higher, particularly at night and in the urban areas that experienced densification. We also show that while both urban and rural temperatures warm up, rural temperatures warm up faster than urban temperatures. Even though urban temperatures remain higher than rural temperatures, the higher warming in rural areas decreases the difference in urban and rural temperatures and the average UHI. This shows that urban and rural areas can respond differently to climate change, and it cannot be assumed that even in the absence of urban growth, that urban and rural areas will experience the same amount of warming with climate change. We further show that the number of hot days and nights per summer doubled with RCP 8.5 for both the Urban Growth and Control scenario, and urban areas experienced more hot nights in the Urban Growth scenario than in the Control scenario.

5.2. The impact of climate change on temperatures and the UHI

Climate change increased temperatures over the entire study area by over 2°C. When urban growth was included, the increases in temperature were higher, particularly for average and minimum temperatures, while maximum temperature increases were similar. These results are similar to those of Argüeso et al. (2014), who found little impact of urbanisation on maximum temperatures. The higher increase in average and minimum temperature with urban growth also occurred in rural areas, where land cover did not change. If urbanisation is not considered in the simulations of future climate, temperatures could be under-estimated, not only across the city, but in nearby rural areas.

While temperatures in urban areas increased, the intensity of the UHI and the frequency of extreme UHIs (UHI intensity > 5°C) decreased in both scenarios with climate change. The decrease in the average UHI was driven by increased warming in rural areas as compared to urban areas, which reduced the urban-rural contrast in temperature at night and increased the difference between urban and rural temperatures during the day. This rural control on the intensity of the urban heat island has also been found for many Indian cities, where irrigation of agriculture is a large factor in the surface UHI (Kumar et al., 2017). The change in UHI intensity found in this study with climate change was most pronounced during the daytime, when the urban cool island strengthened. At night, the UHI intensity decreased. The lower urban warming may be partly, but not entirely, due to the urban areas being closer to the coast than rural areas and the moderating influence of sea-breezes. The higher increase in rural temperatures was also driven by a larger reduction in latent heat flux in rural areas than in urban areas. Under RCP8.5, 2041-2050 exhibited a drying trend, which was reflected in lower relative humidity, soil moisture and precipitation. Incoming longwave and solar radiation also increased due to increased air temperatures and lower cloud cover respectively. With higher incoming energy and less water availability, latent heat flux decreased. Rural areas, which have higher vegetation and higher latent heat flux, were more strongly affected by the reduction in moisture than urban areas.

For many parts of Australia, including the Brisbane area, there is uncertainty regarding future rainfall with climate change (CSIRO & Bureau of Meteorology, 2015; Grose et al., 2015; IPCC, 2014; Walsh et al., 2002). Rainfall may decrease around Brisbane during winter, however these results are uncertain (CSIRO & Bureau of Meteorology, 2015). In areas where a drying trend is projected to occur with climate change, these results show the nocturnal UHI is likely to decrease. However, if rainfall increases, the UHI may intensify instead by the same processes that were found to decrease the UHI with a drying trend. The rural latent heat flux may respond more to the increase in precipitation and increase more than urban latent heat flux. An increase in rural latent heat flux would mean less warming in rural areas than urban areas and an increase in the urban-rural temperature difference and the UHI.

Our findings differ from the results found by (Adachi et al., 2012) in Tokyo, who found urban and rural areas responded similarly to climate change. However, they were similar to the findings of Hamdi et al. (2015) in Brussels, who found the UHI decreased which they attributed to increased rural warming due to soil dryness, as was also found here. Hamdi et al. (2015) also found the winter UHI increased due to changes in wind speed. The seasonal variation in UHI response to climate change was not be studied here due to our focus on summer.

Previous work has suggested a reduction in soil moisture may drive changes in the UHI with climate change, as was found here (Hamdi et al., 2015; Hamdi et al., 2014; Lemonsu et al., 2013; Oleson, 2012). Hamdi et al. (2015) also found decreases in wind speed could increase the winter-time UHI, a process that was not seen here in summer and could not be studied in winter due to the time-frame examined. Hoffmann, Schoetter, et al. (2016) found a moderate increase in the UHI with climate change but attributed this to a regional temperature gradient over the study area. Our results differ from the work of Adachi et al. (2012), who found no climate change impact on the UHI in Tokyo, and that topography was a more important factor than urbanization. Other studies have found differing results, with the impact of climate change on the UHI depending on the urban context (Wiesner et al., 2018). Our study clarifies the processes leading to increased rural warming, which has been lacking in previous work, and confirms a reduction in moisture and rural evapotranspiration can decrease the UHI with climate change. How the UHI changes in each city in response to climate change will depend on the climate impacts on regional climate, particularly cloud cover and rainfall. This study also shows the rural warming and drying trend is enhanced by increasing urban growth. The Urban Growth scenario saw higher increases in maximum temperature in rural areas than the Control scenario, and a larger reduction in rural evapotranspiration and relative humidity in rural areas nearby the city. The drier urban air in the Urban Growth scenario may be intensifying the drying trend in rural areas near the city.

5.3. The impact of climate change and urban growth on heat stress

With RCP8.5, the number of hot days and nights doubled for both scenarios, and the average number of hot night events per summer lasting more than three nights tripled in urban areas. The Urban Growth scenario experienced more hot nights at each urban location than the Control, while there were slightly more hot days in urban areas in the Control. This is possibly due to a shading effect with higher density. The increase in the number hot nights was larger than the reduction in hot days. The biggest increase in number of hot nights per summer occurred in areas which changed from low to medium density, however even areas where land cover did not change, such as the CBD, had an increase in number of hot nights in the Urban Growth scenario. With RCP8.5, the majority of summer nights in medium and high-density areas of the city become ‘hot nights’.

Not only do the number of hot nights increase, but extreme events with consecutive hot nights last longer with climate change, and in the Urban Growth scenario. Consecutive hot nights negatively impact on human health and are linked to increased mortality (Heaviside et al., 2017). Days with minimum temperature over 24°C, which matches the definition of hot nights used here, have been linked to increases in daily mortality for those over 65 of 19-21% (Nicholls et al., 2008). The increase in hot nights with climate change, and increasing duration of hot events, will have serious implications for human health (IPCC, 2014).

We also examined heat stress indices and compared them to thresholds that link heat stress and level of activity. For AT_{sun}, the majority of summer days became 'high' heat stress, while the number of days classified as 'high' heat stress with WBGT and AT_{shade} increased by a factor of 4. Unlike the number of hot nights and days, there was minimal impact of urban growth on heat stress, as it was calculated using average temperature, which increased less with urban growth than minimum temperature. A further effect may be the impacts on heat stress from covariance in abnormally high temperatures and humidity, such that calculating heat stress using minimum or maximum temperatures may give very different results to using average temperature (see also Buzan et al., 2015 for further discussion).

Calculating the heat stress indices with average temperature, not maximum temperature, means dangerous heat stress is not just limited to the hottest part of the day. Short-term exposure to heat while working can increase heat-related illness (Liang et al., 2011). Indoor workers may be able to avoid some of these impacts with air-conditioning, though that will increase outdoor urban temperatures and greenhouse gas emissions (Lundgren & Kjellstrom, 2013; Oleson, 2012). However not everyone works indoors. Outdoor work and activity, even when in the shade, will need to be limited to avoid heat stroke and heat stress (Hanna et al., 2011; Hyatt et al., 2010). As well as health impacts, this will also have negative impacts on worker productivity (Hanna et al., 2011; Hyatt et al., 2010; Lundgren et al., 2013).

5.4. Approach and Limitations

This study used a high-resolution climate model to investigate the impact of urban growth and climate change on the urban heat island and heat stress of a sub-tropical city. The use of a 1 km model allowed us to include multiple urban density types, and to examine the impact on rural areas nearby the city. The limitations of this study are primarily related to the timeframe and processes examined. One process through which climate change could alter the UHI is anthropogenic heat (AH) release. With higher increases in temperatures, air-conditioning would increase, increasing AH and urban temperatures (Bohnenstengel et al., 2014; Lundgren & Kjellstrom, 2013; Oleson, 2012). This process was not examined, but is likely to be important, particularly in high-density areas of the city (Chapman et al., 2016; Quah & Roth, 2012).

This study focussed only on summer temperatures, however given the large increases in temperatures and heat stress, with the majority of summer days being classified as 'high' heat stress, it is likely other seasons will also experience high heat stress (Amengual et al., 2014; Chapman et al., 2017; Fischer & Schär, 2008). This study focused on 10 years only, which is likely not long enough to get an average climatology of rainfall and will not represent the inter-decadal variability in rainfall. This was a necessary limitation given the practical limitations of available resources, and an improvement on previous work which has focussed on time-frames of a year or less (e.g., Adachi et al., 2014; Yang et al., 2016). We believe the results are still useful as it shows the processes by which climate change may affect the UHI. Future work should look at a longer time frame, such as 30 years, to better capture rainfall variability.

All of the heat indices, and the equations used to calculate wet-bulb and globe temperature, have limitations. For example, WBGT responds weakly to wind speed and humidity (Budd, 2008; Smolander et al., 1991; Taylor, 2006). None of the indices chosen consider factors such as age or health, which are important factors in heat stress, and most of the indices assume fit and acclimatized individuals (Konarska et al., 2000; Macpherson, 1962; Smolander et al., 1991). The indices and their threshold values we used here are widely available, which link the index to level of activity and health. The heat stress experienced by unhealthy or older individuals is likely to be higher than indicated by the thresholds calculated here. To address previous limitations in wet-bulb temperature, we have calculated wet-bulb temperature using the Davies-Jones (2008) calculation rather than the Stull (2011) equation, which is inaccurate at higher temperatures (Buzan et al., 2015). We have also used multiple heat stress indices, which weight different aspects of heat stress differently, which has been a weakness in previous work (Buzan et al., 2015). All of these indices show a similar pattern, which gives confidence in the results that however heat stress is measured, it will increase in the future with climate change.

A remaining limitation is that the urban parameters used in this model are based on data from Melbourne, not Brisbane, as this was the best data available for an Australian city. The model validation found a warm bias when simulating Brisbane, particularly in the simulated daily maximum temperatures. We have investigated various potential reasons for the high maximum temperature but have not clearly identified the cause. The bias may be related to the downscaling of the CCAM 100 km resolution simulation forced by ACCESS corrected sea surface temperatures. However, ACCESS sea surface temperatures are necessary to make a prediction of the future Brisbane climate under a global warming scenario and the corrected sea surface temperatures generally improves the simulated present-day climate. Nevertheless, in future work we will consider sea surface temperatures from other GCMs to determine their impact on the simulated Brisbane climate. Future work will also improve the input data available for the model parameters and consider processes not examined here, such as changes to anthropogenic heat release.

5.5. Implications for urban planning and human health

Brisbane already faces health risks from heat stress (Tong et al., 2010), which will intensify with urban growth and climate change. Even though the intensity of the UHI and the number of extreme UHIs decrease with climate change, urban and rural temperatures both increases, and high-intensity UHIs still occur, and occurred twice as often in the Urban Growth scenario

Accepted Article

as in the Control scenario. Day-time heat stress and number of hot days increased for urban areas, and the number of hot nights remains much higher for urban areas than for rural areas. This means urban residents will face increasing heat stress risks, particularly if a high-intensity (> 5°C) UHI occurs, which occurred 9 days per summer in the Control scenario, and 15 days per summer in the Urban Growth scenario in 2041-2050. Outdoor workers will face high health risks, even in shaded conditions. During an increasing number of summer days, outdoor work and sport will need to be limited to prevent heat stress.

Since 2005, humanity has been following the RCP8.5 emissions path (Sanderson et al., 2016). Rapid mitigation of climate change is vital to avoid the temperature impacts associated with this scenario, though it is clear now not all climate change impacts can be avoided and adaptation to higher temperatures is also necessary (Pielke et al., 2007; Rogelj et al., 2016; Sanderson et al., 2016). Despite the reduction in the UHI found in this scenario, caused by a slight reduction in the night-time UHI and an increase in the urban cool island during the day, the night time UHI remains high and with the increase in temperatures, urban residents face higher overall heat stress risks in 2041-2050 than in the present day. Urban planners need to seriously consider the heat stress urban residents will face in the future, and options to mitigate the UHI, so that urban design does not exacerbate the temperature increases from climate change (Grimmond, 2007; Heaviside et al., 2017; Li & Bou-Zeid, 2013). Less developed tropical and sub-tropical regions, particularly those predicted to have high urban growth, such as Africa (Seto et al., 2012), may be particularly vulnerable to future increases in the UHI, due to limited resources to respond to increased heat stress risks (Hyatt et al., 2010; IPCC, 2014; Kjellstrom, 2009). Given limited resources, planners should focus on areas of the city most at risk of heat stress, either due to socio-economic status or urban design (Hajat et al., 2010; Laaidi et al., 2012; Luber & McGeehin, 2008). A more detailed and realistic land-cover map would enable planners to identify at-risk suburbs and focus mitigation efforts on them.

Heat-warning systems, cool-roofs and increased greening can be effective in reducing the intensity of the UHI (Bowler et al., 2010; Coutts et al., 2013; Heaviside et al., 2017). Research in Australia has found mortality could be reduced by between 5-28% by an increase in vegetation from 15-33% in high density areas (Chen et al., 2014). Our model did not include irrigation in urban areas, so it could be considered a 'worst-case' scenario for the UHI intensity. However, the drying trend means mitigation through increased greening may have limited effect without irrigation, and water availability may become an issue, particularly in a drought-prone country like Australia (Coutts et al., 2013).

We also found the urban heat island effect spreads out to neighbouring areas. This means even areas which do have green space may be negatively affected by nearby high-density low-green space areas. The wider impacts of inner-city development decisions on surrounding suburbs need to be considered by planners. Finally, the Urban Growth scenario considered here was not an extreme scenario. Over half of the urban area was densified, and this only included a reduction in green space of 11% and increase in building height of 2 m. Actual urban densification may be much higher than this, and so the UHI and night-time heat stress could be higher. The health risks urban and rural residents will face in the future due to climate change will be high; urban planners need to ensure urban growth does not magnify these risks any further.

6. Conclusion

We examined the impact of climate change and urban growth on the UHI of Brisbane, a sub-tropical city in Australia, during summer. We found higher increases in average and minimum temperatures when both urban growth and climate change were considered. While temperatures increased in both urban and rural areas, and urban temperatures remained higher than rural temperatures, rural temperatures warmed up more, decreasing the difference between urban and rural temperatures at night, and increasing the urban cool island during the day. This led to an overall decrease in the average UHI. The higher rural warming was due to a drying-trend. This rural warming was more pronounced with urban growth, potentially due to the more coastal location of urban areas and the dry-urban air affecting nearby rural areas. Whether regions will get drier or wetter with climate change will affect the urban-rural temperature balance and the UHI intensity. Future work should also focus on other processes important to the UHI - climate interaction, such as anthropogenic heat release, which may increase or decrease the UHI depending on whether the increase air-conditioning is higher than decrease in heating in winter.

We forecast major increases in heat stress, duration of heat events, and number of hot days and nights with climate change and urban growth. The number of hot days and nights doubled, and dangerous heat stress occurred every summer, even in shady conditions. These results mean outdoor work and sport will need to be limited in duration to reduce the risks of heat stress. We only examined the summer season, but given the large increases in heat stress, it is likely heat stress will be an issue in other seasons as well. Mitigation of urban temperatures will become more vital in the future and urban planners need to consider the temperature effects of development decisions to ensure they are not contributing to the heat stress burden urban residents will already face with climate change.

Acknowledgements

This research was undertaken with the assistance of resources and services from the National Computational Infrastructure (NCI), which is supported by the Australian Government. We thank the Brisbane City Council for providing Brisbane zoning data. SC was supported by an

Australian Postgraduate Award. This project was supported by Australian Research Council Discovery Project DP160102107.

Supporting Information

Table S1: Missing data and years open for weather stations used in model validation.

Figure S1: Hourly variation in urban and rural temperatures in the present day (1991-2000) and medium term (2041-2050).

Figure S2: Precipitation and cloud cover in Control present day (1991-2000) and change in precipitation and cloud cover in the medium term (2041-2050).

Figure S3: Change in soil moisture wetness fraction for Control and Urban Growth scenarios between the present day and the medium term.

Figure S4: Difference in incoming and net solar and longwave radiation for Control and Urban Growth scenarios between the present day and the medium term.

References

Adachi, S. A., Kimura, F., Kusaka, H., Duda, M. G., Yamagata, Y., Seya, H., . . . Aoyagi, T. (2014). Moderation of Summertime Heat Island Phenomena via Modification of the Urban Form in the Tokyo Metropolitan Area. Journal of Applied Meteorology and Climatology, 53(8), 1886-1900. doi:10.1175/JAMC-D-13-0194.1

Adachi, S. A., Kimura, F., Kusaka, H., Inoue, T., & Ueda, H. (2012). Comparison of the Impact of Global Climate Changes and Urbanization on Summertime Future Climate in the Tokyo Metropolitan Area. Journal of Applied Meteorology and Climatology, 51(8), 1441-1454. doi:http://dx.doi.org/10.1175/JAMC-D-11-0137.1

Althor, G., Watson, J. E. M., & Fuller, R. A. (2016). Global mismatch between greenhouse gas emissions and the burden of climate change. Scientific reports, 6, 20281. doi:10.1038/srep20281

Amengual, A., Homar, V., Romero, R., Brooks, H. E., Ramis, C., Gordaliza, M., & Alonso, S. (2014). Projections of heat waves with high impact on human health in Europe. Global and Planetary Change, 119, 71-84. doi:http://doi.org/10.1016/j.gloplacha.2014.05.006

Argüeso, D., Evans, J., Fita, L., & Bormann, K. (2014). Temperature response to future urbanization and climate change. Climate Dynamics, 42(7-8), 2183-2199. doi:10.1007/s00382-013-1789-6

Argüeso, D., Evans, J. P., Pitman, A. J., & Di Luca, A. (2015). Effects of City Expansion on Heat Stress under Climate Change Conditions. PLoS ONE, 10(2), e0117066. doi:10.1371/journal.pone.0117066

Arnfield, A. J. (2003). Two decades of urban climate research: a review of turbulence, exchanges of energy and water, and the urban heat island. International Journal of Climatology, 23(1), 1-26. doi:10.1002/joc.859

Australian Bureau of Meteorology. (2010). Thermal comfort observations. Retrieved from http://www.bom.gov.au/info/thermal_stress/

Australian Bureau of Statistics. (2013). Population Projections, Australia, 2012 (base) to 2101. Retrieved from http://www.abs.gov.au/AUSSTATS/abs@.nsf/mf/3222.0

Barriopedro, D., Fischer, E. M., Luterbacher, J., Trigo, R. M., & García-Herrera, R. (2011). The Hot Summer of 2010: Redrawing the Temperature Record Map of Europe. Science, 332(6026), 220-224. doi:10.1126/science.1201224

Bi, D. H., Dix, M., Marsland, S. J., O'Farrell, S., Rashid, H. A., Uotila, P., . . . Puri, K. (2013). The ACCESS coupled model: description, control climate and evaluation. Australian Meteorological and Oceanographic Journal, 63(1), 41-64. doi:10.22499/2.6301.004

Bohnenstengel, S. I., Hamilton, I., Davies, M., & Belcher, S. E. (2014). Impact of anthropogenic heat emissions on London's temperatures. Quarterly Journal of the Royal Meteorological Society, 140(679), 687-698. doi:10.1002/qj.2144

Bonan, G. (2008). Ecological Climatology: Concepts and Applications (2nd ed.). New York: Cambridge University Press.

Bowler, D. E., Buyung-Ali, L., Knight, T. M., & Pullin, A. S. (2010). Urban greening to cool towns and cities: A systematic review of the empirical evidence. Landscape and Urban Planning, 97(3), 147-155. doi:http://dx.doi.org/10.1016/j.landurbplan.2010.05.006

Brake, R., & Bates, G. (2002). A valid method for comparing rational and empirical heat stress indices. Annals of Occupational Hygiene, 46(2), 165-174. doi:10.1093/annhyg/mef030

Brisbane City Council. (2014). Brisbane City Plan 2014. Brisbane Retrieved from http://eplan.brisbane.qld.gov.au/

Budd, G. M. (2008). Wet-bulb globe temperature (WBGT)—its history and its limitations. Journal of Science and Medicine in Sport, 11(1), 20-32. doi:10.1016/j.jsams.2007.07.003

Bureau of Meteorology. (2017). Summary statistics BRISBANE. Retrieved from http://www.bom.gov.au/climate/averages/tables/cw_040913.shtml

Buzan, J. R., Oleson, K., & Huber, M. (2015). Implementation and comparison of a suite of heat stress metrics within the Community Land Model version 4.5. Geosci. Model Dev., 8(2), 151-170. doi:10.5194/gmd-8-151-2015

Chang, C.-R., Li, M.-H., & Chang, S.-D. (2007). A preliminary study on the local cool-island intensity of Taipei city parks. Landscape and Urban Planning, 80(4), 386-395. doi:http://dx.doi.org/10.1016/j.landurbplan.2006.09.005

Chapman, S., Thatcher, M., Salazar, A., Watson, J. E. M., & McAlpine, C. A. (2018). The effect of urban density and vegetation cover on the heat island of a subtropical city. Journal of Applied Meteorology and Climatology. doi:10.1175/JAMC-D-17-0316.1

Chapman, S., Watson, J. E. M., & McAlpine, C. A. (2016). Large seasonal and diurnal anthropogenic heat flux across four Australian cities. Journal of Southern Hemisphere Earth Systems Science, 66(3), 342-360.

Chapman, S., Watson, J. E. M., Salazar, A., Thatcher, M., & McAlpine, C. A. (2017). The impact of urbanization and climate change on urban temperatures: a systematic review. Landscape Ecology, 32(10), 1921-1935. doi:10.1007/s10980-017-0561-4

Chen, D., Thatcher, M., Wang, X., Barnett, G., Kachenko, A., & Prince, R. (2015). Summer cooling potential of urban vegetation—a modeling study for Melbourne, Australia. AIMS Environmental Science, 2(3), 648-667. doi:10.3934/environsci.2015.3.648

Chen, D., Wang, X., Thatcher, M., Barnett, G., Kachenko, A., & Prince, R. (2014). Urban vegetation for reducing heat related mortality. Environmental Pollution, 192(0), 275-284. doi:http://dx.doi.org/10.1016/j.envpol.2014.05.002

Chouinard, C., Béland, M., & McFarlane, N. (1986). A simple gravity wave drag parametrization for use in medium- range weather forecast models. Atmosphere-Ocean, 24(2), 91-110. doi:10.1080/07055900.1986.9649242

Chun, B., & Guldmann, J. M. (2014). Spatial statistical analysis and simulation of the urban heat island in high-density central cities. Landscape and Urban Planning, 125(0), 76-88. doi:http://dx.doi.org/10.1016/j.landurbplan.2014.01.016

Clarke, J. F. (1972). Some effects of the urban structure on heat mortality. Environmental Research, 5(1), 93-104. doi:http://dx.doi.org/10.1016/0013-9351(72)90023-0

Coates, L., Haynes, K., O'Brien, J., McAneney, J., & de Oliveira, F. D. (2014). Exploring 167 years of vulnerability: An examination of extreme heat events in Australia 1844–

2010. Environmental Science & Policy, 42, 33-44. doi:http://dx.doi.org/10.1016/j.envsci.2014.05.003

Coutts, A. M., Beringer, J., & Tapper, N. J. (2007). Impact of Increasing Urban Density on Local Climate: Spatial and Temporal Variations in the Surface Energy Balance in Melbourne, Australia. Journal of Applied Meteorology and Climatology, 46(4), 477-480,482-493.

Coutts, A. M., Tapper, N. J., Beringer, J., Loughnan, M., & Demuzere, M. (2013). Watering our cities: The capacity for Water Sensitive Urban Design to support urban cooling and improve human thermal comfort in the Australian context. Progress in Physical Geography, 37(1), 2-28. doi:10.1177/0309133312461032

CSIRO, & Bureau of Meteorology. (2015). Climate change in Australia: Projections for Australia's NRM Regions. Retrieved from Australia:

d'Ambrosio Alfano, F. R., Malchaire, J., Palella, B. I., & Riccio, G. (2014). WBGT Index Revisited After 60 Years of Use. Annals of Occupational Hygiene, 58(8), 955-970. doi:10.1093/annhyg/meu050

Davies-Jones, R. (2008). An Efficient and Accurate Method for Computing the Wet-Bulb Temperature along Pseudoadiabats. Monthly Weather Review, 136(7), 2764-2785. doi:10.1175/2007mwr2224.1

Department of Natural Resources, Mines and Energy. (2013). Digital elevation models 25metre by catchment areas series.

Environmental Protection Agency. (2016). Climate Change Indicators in the United States: Heat-Related Deaths. Retrieved from https://www.epa.gov/sites/production/files/2016-08/documents/print_heat-deaths-2016.pdf

Epstein, Y., & Moran, D. S. (2006). Thermal Comfort and the Heat Stress Indices. Industrial Health, 44(3), 388-398. doi:10.2486/indhealth.44.388

Fischer, E. M., & Schär, C. (2008). Future changes in daily summer temperature variability: driving processes and role for temperature extremes. Climate Dynamics, 33(7), 917. doi:10.1007/s00382-008-0473-8

Fouillet, A., Rey, G., Wagner, V., Laaidi, K., Empereur-Bissonnet, P., Le Tertre, A., . . . Hémon, D. (2008). Has the impact of heat waves on mortality changed in France since the European heat wave of summer 2003? A study of the 2006 heat wave. International journal of epidemiology, 37(2), 309-317. doi:10.1093/ije/dym253

Gedzelman, S. D., Austin, S., Cermak, R., Stefano, N., Partridge, S., Quesenberry, S., & Robinson, D. A. (2003). Mesoscale aspects of the Urban Heat Island around New York City. Theoretical and Applied Climatology, 75(1-2), 29-42. doi:10.1007/s00704-002-0724-2

Global Land Cover Facility. (2018). MODIS Land Cover. Retrieved from http://glcf.umd.edu/data/lc/

Grimmond, C. S. B. (2007). Urbanization and global environmental change: local effects of urban warming. Geographical Journal, 173(1), 83-88. doi:10.1111/j.1475-4959.2007.232_3.x

Grose, M., Bhend, J., Argueso, D., Ekstrom, M., Dowdy, A., Hoffmann, P., . . . Timbal, B. (2015). Comparison of various climate change projections of eastern Australian rainfall. Aust. Meteorol. Oceanogr. J., 65(1), 72-89. doi:10.22499/2.6501.006

Hajat, S., O'Connor, M., & Kosatsky, T. (2010). Health effects of hot weather: from awareness of risk factors to effective health protection. The Lancet, 375(9717), 856-863. doi:10.1016/S0140-6736(09)61711-6

Hajizadeh, R., Farhang, D. S., Golbabaei, F., Jafari, S. M., & Karajizadeh, M. (2017). Offering a model for estimating black globe temperature according to meteorological measurements. Meteorological applications, 24(2), 303-307. doi:doi:10.1002/met.1631

Hamdi, R., Giot, O., De Troch, R., Deckmyn, A., & Termonia, P. (2015). Future climate of Brussels and Paris for the 2050s under the A1B scenario. Urban Climate, 12, 160-182. doi:https://doi.org/10.1016/j.uclim.2015.03.003

Hamdi, R., Van de Vyver, H., De Troch, R., & Termonia, P. (2014). Assessment of three dynamical urban climate downscaling methods: Brussels's future urban heat island under an A1B emission scenario. International Journal of Climatology, 34(4), 978-999. doi:10.1002/joc.3734

Hanna, E. G., Kjellstrom, T., Bennett, C., & Dear, K. (2011). Climate Change and Rising Heat: Population Health Implications for Working People in Australia. Asia-Pacific Journal of Public Health, 23(2), 14S-26S. doi:10.1177/1010539510391457

Hayhoe, K., Sheridan, S., Kalkstein, L., & Greene, S. (2010). Climate Change, Heat Waves, and Mortality Projections for Chicago. Journal of Great Lakes Research, 36(2), 65-73. doi:10.1016/j.jglr.2009.12.009

Heaviside, C., Macintyre, H., & Vardoulakis, S. (2017). The Urban Heat Island: Implications for Health in a Changing Environment. Current Environmental Health Reports. doi:10.1007/s40572-017-0150-3

Hoffmann, P., Katzfey, J. J., McGregor, J. L., & Thatcher, M. (2016). Bias and variance correction of sea surface temperatures used for dynamical downscaling. Journal of Geophysical Research: Atmospheres, 121(21), 12,877-812,890. doi:10.1002/2016JD025383

Hoffmann, P., Krueger, O., & Schlünzen, K. H. (2012). A statistical model for the urban heat island and its application to a climate change scenario. International Journal of Climatology, 32(8), 1238-1248. doi:10.1002/joc.2348

Hoffmann, P., Schoetter, R., & Schlünzen, K. H. (2016). Statistical-dynamical downscaling of the urban heat island in Hamburg, Germany. Meteorologische Zeitschrift, 27(2). doi:10.1127/metz/2016/0773

Holtslag, A. A. M., & Boville, B. A. (1993). Local Versus Nonlocal Boundary-Layer Diffusion in a Global Climate Model. Journal of Climate, 6(10), 1825-1842. doi:10.1175/1520-0442(1993)006<1825:LVNBLD>2.0.CO;2

Hyatt, O. M., Lemke, B., & Kjellstrom, T. (2010). Regional maps of occupational heat exposure: past, present, and potential future. Global Health Action, 3(1), 5715. doi:10.3402/gha.v3i0.5715

IPCC. (2014). Climate Change 2014: Impacts, Adaptation, and Vulnerability. Part A: Global and Sectoral Aspects. Contribution of Working Group II to the Fifth Assessment Report of the Intergovernmental Panel on Climate Change [Field, C.B., V.R. Barros, D.J. Dokken, K.J. Mach, M.D. Mastrandrea, T.E. Bilir, M. Chatterjee, K.L. Ebi, Y.O. Estrada, R.C. Genova, B. Girma, E.S. Kissel, A.N. Levy, S. MacCracken, P.R. Mastrandrea, and L.L. White (eds.)]. Cambridge, United Kingdom and New York, NY, USA: Cambridge University Press.

Kim, Y.-M., Kim, S., Cheong, H.-K., & Kim, E.-H. (2011). Comparison of Temperature Indexes for the Impact Assessment of Heat Stress on Heat-Related Mortality. Environmental Health and Toxicology, 26, e2011009. doi:10.5620/eht.2011.26.e2011009

Kjellstrom, T. (2009). Climate change, direct heat exposure, health and well-being in low and middle-income countries. Global Health Action, 2, 10.3402/gha.v3402i3400.1958. doi:10.3402/gha.v2i0.1958

Konarska, M., Soltynski, K., & Marszalek, A. (2000). Problems in Evaluation Heat Stress Risk of Women Workers Using the WBGT Index. Human Factors and Ergonomics Society Annual Meeting Proceedings, 44(35), 453-453.

Kowalczyk, E., Wang, Y. P., Law, R. M., Davies, H. L., McGregor, J. L., & Abramowitz, G. (2006). The CSIRO Atmosphere Biosphere Land Exchange (CABLE) model for use in climate models and as an offline model. Retrieved from Aspendal, Vic, Australia:

Kumar, R., Mishra, V., Buzan, J., Kumar, R., Shindell, D., & Huber, M. (2017). Dominant control of agriculture and irrigation on urban heat island in India. Scientific reports, 7(1), 14054. doi:10.1038/s41598-017-14213-2

Laaidi, K., Zeghnoun, A., Dousset, B., Bretin, P., Vandentorren, S., Giraudet, E., & Beaudeau, P. (2012). The Impact of Heat Islands on Mortality in Paris during the August 2003 Heat Wave. Environmental Health Perspectives, 120(2), 254-259. doi:10.1289/ehp.1103532

Lemonsu, A., Kounkou-Arnaud, R., Desplat, J., Salagnac, J. L., & Masson, V. (2013). Evolution of the Parisian urban climate under a global changing climate. Climatic Change, 116(3-4), 679-692. doi:10.1007/s10584-012-0521-6

Li, D., & Bou-Zeid, E. (2013). Synergistic Interactions between Urban Heat Islands and Heat Waves: The Impact in Cities Is Larger than the Sum of Its Parts. Journal of Applied Meteorology and Climatology, 52(9), 2051-2064. doi:10.1175/jamc-d-13-02.1

Liang, C., Zheng, G., Zhu, N., Tian, Z., Lu, S., & Chen, Y. (2011). A new environmental heat stress index for indoor hot and humid environments based on Cox regression. Building and Environment, 46(12), 2472-2479. doi:https://doi.org/10.1016/j.buildenv.2011.06.013

Lin, Y.-L., Farley, R. D., & Orville, H. D. (1983). Bulk Parameterization of the Snow Field in a Cloud Model. Journal of Climate and Applied Meteorology, 22(6), 1065-1092. doi:10.1175/1520-0450(1983)022<1065:bpotsf>2.0.co;2

Luber, G., & McGeehin, M. (2008). Climate Change and Extreme Heat Events. American Journal of Preventive Medicine, 35(5), 429-435. doi:10.1016/j.amepre.2008.08.021

Luhar, A. K., Thatcher, M., & Hurley, P. J. (2014). Evaluating a building-averaged urban surface scheme in an operational mesoscale model for flow and dispersion. Atmospheric Environment, 88, 47-58. doi:10.1016/j.atmosenv.2014.01.059

Lundgren, K., & Kjellstrom, T. (2013). Sustainability Challenges from Climate Change and Air Conditioning Use in Urban Areas. Sustainability, 5(7), 3116-3128. doi:10.3390/su5073116

Lundgren, K., Kuklane, K., Gao, C., & Holmer, I. (2013). Effects of Heat Stress on Working Populations when Facing Climate Change. Industrial Health, 51(1), 3-15.

Macpherson, R. K. (1962). The Assessment of the Thermal Environment a Review. British journal of industrial medicine, 19(3), 151-164.

Masson, V. (2000). A Physically-Based Scheme For The Urban Energy Budget In Atmospheric Models. Boundary-Layer Meteorology, 94(3), 357-397. doi:10.1023/A:1002463829265

McCarthy, M. P., Best, M. J., & Betts, R. A. (2010). Climate change in cities due to global warming and urban effects. Geophysical Research Letters, 37(9). doi:10.1029/2010GL042845

McGregor, J. L. (2003). A new convection scheme using a simple closure. Current issues in the parameterization of convection(93), 33-36.

McGregor, J. L., & Dix, M. R. (2008). An Updated Description of the Conformal-Cubic Atmospheric Model. In (pp. 51-75). New York, NY: Springer New York.

McGregor, J. L., Gordon, H. B., Watterson, I. G., Dix, M. R., & Rotstayn, L. D. (1993). The CSIRO 9-level Atmospheric General Circulation Model. Retrieved from Aspendal, Vic, Australia:

Medina-Ramón, M., & Schwartz, J. (2007). Temperature, Temperature Extremes, and Mortality: A Study of Acclimatisation and Effect Modification in 50 US Cities. Occupational and Environmental Medicine, 64(12), 827-833. doi:10.2307/27733049

Morabito, M., Crisci, A., Messeri, A., Capecchi, V., Modesti, P. A., Gensini, G. F., & Orlandini, S. (2014). Environmental Temperature and Thermal Indices: What Is the Most Effective Predictor of Heat-Related Mortality in Different Geographical Contexts? SCIENTIFIC WORLD JOURNAL, 2014, 1-15. doi:10.1155/2014/961750

National Weather Service. (2018). What is the heat index? Retrieved from https://www.weather.gov/ama/heatindex

Nicholls, N., Skinner, C., Loughnan, M., & Tapper, N. (2008). A simple heat alert system for Melbourne, Australia. International Journal of Biometeorology, 52(5), 375-384. doi:10.1007/s00484-007-0132-5

Oke, T. R. (1973). City size and the urban heat island. Atmospheric Environment (1967), 7(8), 769-779. doi:http://dx.doi.org/10.1016/0004-6981(73)90140-6

Oke, T. R. (1982). The energetic basis of the urban heat island. Quarterly Journal of the Royal Meteorological Society, 108(455), 1-24. doi:10.1002/qj.49710845502

Oke, T. R. (1995). The heat island of the urban boundary layer: characteristics, causes and effects. In J. E. Cermak, A. G. Davenport, E. J. Plate, & D. X. Viegas (Eds.), Wind Climate in Cities (pp. 81-107): Springer Netherlands.

Oleson, K. (2012). Contrasts between Urban and Rural Climate in CCSM4 CMIP5 Climate Change Scenarios. Journal of Climate, 25(5), 1390-1412. doi:http://dx.doi.org/10.1175/JCLI-D-11-00098.1

Ooka, R., Minami, Y., Sakoi, T., Tsuzuki, K., & Rijal, H. B. (2010). Improvement of sweating model in 2-Node Model and its application to thermal safety for hot environments. Building and Environment, 45(7), 1565-1573. doi:http://dx.doi.org/10.1016/j.buildenv.2009.12.012

Parker, D. E. (2010). Urban heat island effects on estimates of observed climate change. Wiley Interdisciplinary Reviews: Climate Change, 1(1), 123-133. doi:http://dx.doi.org/10.1002/wcc.021

Pielke, R., Jr., Prins, G., Rayner, S., & Sarewitz, D. (2007). Climate change 2007: Lifting the taboo on adaptation. Nature, 445(7128), 597-598.

Quah, A. K. L., & Roth, M. (2012). Diurnal and weekly variation of anthropogenic heat emissions in a tropical city, Singapore. Atmospheric Environment, 46, 92-103. doi:10.1016/j.atmosenv.2011.10.015

Ren, Z., Wang, X., Chen, D., Wang, C., & Thatcher, M. (2014). Constructing weather data for building simulation considering urban heat island. Building Services Engineering Research & Technology, 35(1), 69-82. doi:http://dx.doi.org/10.1177/0143624412467194

Robine, J.-M., Cheung, S. L. K., Le Roy, S., Van Oyen, H., Griffiths, C., Michel, J.-P., & Herrmann, F. R. (2008). Death toll exceeded 70,000 in Europe during the summer of 2003. Comptes Rendus Biologies, 331(2), 171-178. doi:https://doi.org/10.1016/j.crvi.2007.12.001

Rogelj, J., den Elzen, M., Höhne, N., Fransen, T., Fekete, H., Winkler, H., . . . Meinshausen, M. (2016). Paris Agreement climate proposals need a boost to keep warming well below 2 °C. Nature, 534(7609), 631-639. doi:10.1038/nature18307

Rotstayn, L. D. (1997). A physically based scheme for the treatment of stratiform clouds and precipitation in large-scale models. I: Description and evaluation of the microphysical processes. Quarterly Journal of the Royal Meteorological Society, 123(541), 1227-1282. doi:10.1002/qj.49712354106

Sailor, D. J., & Lu, L. (2004). A top–down methodology for developing diurnal and seasonal anthropogenic heating profiles for urban areas. Atmospheric Environment, 38(17), 2737-2748. doi:http://dx.doi.org/10.1016/j.atmosenv.2004.01.034

Sanderson, B. M., O'Neill, B. C., & Tebaldi, C. (2016). What would it take to achieve the Paris temperature targets? Geophysical Research Letters, 43(13), 7133-7142. doi:10.1002/2016GL069563

Schwarzkopf, M. D., & Fels, S. B. (1991). The simplified exchange method revisited: An accurate, rapid method for computation of infrared cooling rates and fluxes. Journal of Geophysical Research: Atmospheres, 96(D5), 9075-9096. doi:10.1029/89JD01598

Schwarzkopf, M. D., & Ramaswamy, V. (1999). Radiative effects of CH4, N2O, halocarbons and the foreign- broadened H2O continuum: A GCM experiment. Journal of Geophysical Research: Atmospheres, 104(D8), 9467-9488. doi:doi:10.1029/1999JD900003

Seto, K. C., Güneralp, B., & Hutyra, L. R. (2012). Global forecasts of urban expansion to 2030 and direct impacts on biodiversity and carbon pools. Proceedings of the National Academy of Sciences, 109(40), 16083-16088. doi:10.1073/pnas.1211658109

Sharifi, E., & Lehmann, S. (2014). Comparative Analysis of Surface Urban Heat Island Effect in Central Sydney. Journal of Sustainable Development, 7(3), 23-34.

Sherwood, S. C., Huber, M., & Emanuel, K. A. (2010). An adaptability limit to climate change due to heat stress. Proceedings of the National Academy of Sciences of the United States of America, 107(21), 9552-9555. doi:10.2307/25681637

Smolander, J., Ilmarinen, R., & Korhonen, O. (1991). An evaluation of heat stress indices (ISO 7243, ISO/DIS 7933) in the prediction of heat strain in unacclimated men. International Archives of Occupational and Environmental Health, 63(1), 39-41. doi:10.1007/BF00406196

Sports Medicine Australia. (2007). Hot weather guidelines for sporting clubs and associations and the physically active. Retrieved from http://sma.org.au/resources-advice/policies-guidelines/hot-weather/

Steadman, R. G. (1984). A universal scale of apparent temperature. Journal of Climate & Applied Meteorology, 23(12), 1674-1687.

Stull, R. (2011). Wet-Bulb Temperature from Relative Humidity and Air Temperature. Journal of Applied Meteorology and Climatology, 50(11), 2267-2269. doi:10.1175/jamc-d-11-0143.1

Taha, H. (1997). Urban climates and heat islands: albedo, evapotranspiration, and anthropogenic heat. Energy & Buildings, 25(2), 99-103. doi:10.1016/S0378-7788(96)00999-1

Taylor, N. A. S. (2006). Challenges to Temperature Regulation When Working in Hot Environments. Industrial Health, 44(3), 331-344. doi:10.2486/indhealth.44.331

Thatcher, M., & Hurley, P. (2012). Simulating Australian Urban Climate in a Mesoscale Atmospheric Numerical Model. Boundary-Layer Meteorology, 142(1), 149-175. doi:10.1007/s10546-011-9663-8

Tong, S., Ren, C., & Becker, N. (2010). Excess deaths during the 2004 heatwave in Brisbane, Australia. International Journal of Biometeorology, 54(4), 393-400. doi:10.1007/s00484-009-0290-8

Unger, J. (2009). Connection between urban heat island and sky view factor approximated by a software tool on a 3D urban database. International Journal of Environment and Pollution, 36(1-3), 59-80. doi:10.1504/IJEP.2009.021817

United Nations. (2014). World Urbanization Prospects: The 2014 Revision - Highlights. Retrieved from New York:

Walsh, K., Cai, W., Hennessy, K., Jones, R., McInnes, K., Nguyen, K., . . . Whetton, P. (2002). Climate Change in Queensland under Enhanced Greenhouse Conditions. Retrieved from Aspendale, Vic, Australia:

Wiesner, S., Bechtel, B., Fischereit, J., Gruetzun, V., Hoffmann, P., Leitl, B., . . . Thomsen, S. (2018). Is It Possible to Distinguish Global and Regional Climate Change from Urban Land Cover Induced Signals? A Mid-Latitude City Example. Urban Science, 2(1), 12.

Wilby, R. L. (2008). Constructing climate change scenarios of urban heat island intensity and air quality. Environment and Planning B: Planning and Design, 35(5), 902-919.

World Meteorological Organization. (2016). WMO Statement on the status of the global climate in 2015. Retrieved from Geneva:

Yang, L., Niyogi, D., Tewari, M., Aliaga, D., Chen, F., Tian, F., & Ni, G. (2016). Contrasting impacts of urban forms on the future thermal environment: example of Beijing metropolitan area. Environmental Research Letters, 11(3), 034018.

Yow, D. M. (2007). Urban Heat Islands: Observations, Impacts, and Adaptation. Geography Compass, 1(6), 1227-1251. doi:http://dx.doi.org/10.1111/j.1749-8198.2007.00063.x

Zwiers, F. W., & Storch, H. v. (1995). Taking Serial Correlation into Account in Tests of the Mean. Journal of Climate, 8(2), 336-351. doi:10.1175/1520-0442(1995)008

Table 1: Physics schemes used in the Conformal Cubic Atmospheric Model

Physical Options	Schemes
Cloud microphysics	Liquid and ice-water microphysics scheme of Rotstayn (1997). Snow and graupel scheme of Lin et al. (1983)
Convective parameterization	Mass-flux cumulus convection scheme (McGregor, 2003; McGregor & Dix, 2008)
Radiation scheme	Geophysical Fluid Dynamics Laboratory (GFDL) parametrization for short and long-wave radiation (Schwarzkopf & Fels, 1991; Schwarzkopf & Ramaswamy, 1999)
Gravity wave drag	Chouinard et al. (1986)
Boundary layer	Local Richardson number (McGregor et al., 1993) and nonlocal vertical mixing (Holtslag & Boville, 1993)
Land surface model	CABLE land surface scheme (Kowalczyk et al., 2006)
Urban model	Australian Town Energy Budget (Thatcher & Hurley, 2012)

Table 2: Details of the land cover scenarios used in the climate modelling experiments. Both experiments were run under RCP8.5.

Name	Land Cover Scenario	Climate Scenario	Present day	Mid term
Control	MODIS 2001 data with high-density CBD area added	RCP8.5	1991 – 2000	2041 – 2050
Urban Growth	Control land cover, with the addition of medium-density area within inner half of the city	RCP8.5	1991 – 2000	2041 – 2050

Table 3: Characteristics of the urban categories (high, medium and low density) used in ATEB, Australian Town Energy Budget Model.

Category	Urban - high	Urban - medium	Urban - low
Building height (m)	18	8	6
Building fraction	65%	46%	45%
Green space fraction	5%	34%	45%
Height/width ratio	2	0.6	0.4
Roof albedo	0.2	0.2	0.2
Wall albedo	0.3	0.3	0.3
Road albedo	0.1	0.1	0.1
Vegetation roughness length	0.1	0.1	0.1

Table 4: Bias and for the Control scenario as compared to weather observations for minimum, maximum and average temperature, and relative humidity (RH) and 10m wind speed (U10). * indicates stations open the entire time period. Amberley = 040004, Archerfield = 040211, B. Aero 1 = 040223, B. Aero 2 = 040842, Samford = 040241, Logan = 040854, Redcliffe = 040697. Samford and Logan excluded from average temperature calculations due to a lack of hourly data. Amberley average temperature only compared to model data from February 1992 onwards, due to insufficient hourly data prior to that. Temperature data from CCAM bias corrected based on elevation difference between CCAM and barometer height of weather station.

Station	Min	Max	Ave	U10	RH
Amberley	-1.6	3.0	0.6	1.1	2.7
Archerfield*	-0.8	2.4	0.5	-0.1	-2.4
B. Aero 1	1.4	0.9	1.0	-0.2	-4.6
Samford	>0.1	1.2	-	1.2	2.0
Redcliffe	-	-	-	1.5	-
B. Aero 2	1.0	1.1	0.9	-0.5	-3.2
Logan	-5.5	3.7	-	0.3	9.5
Mean	-0.9	2.0	0.7	0.5	0.7

Table 5: Change (midterm–present day) in seasonal average, minimum and maximum summer temperatures in rural areas and urban for the Control and Urban Growth scenarios as compared to the Control present day scenario. Only rural areas within the same elevation range as Brisbane city included in calculation of rural temperature change. Low density refers to areas which were low density in both scenarios. Medium Density refers to areas which were medium density in the Urban Growth scenario, but low density in the Control scenario. Spatial standard deviation in brackets. The CBD standard deviation is low due to the small spatial area it covers.

Location	Control			Urban Growth		
	Tave	Tmin	Tmax	Tave	Tmin	Tmax
Rural	2.8	2.5	3.4	2.8	2.5	3.5
	(0.2)	(0.1)	(0.4)	(0.2)	(0.2)	(0.5)
Low density	2.5	2.4	2.8	2.5	2.5	2.8
	(0.2)	(0.1)	(0.4)	(0.3)	(0.2)	(0.5)
Medium Density	2.3	2.4	2.6	2.5	2.8	2.5
	(0.2)	(0.1)	(0.3)	(0.2)	(0.2)	(0.3)
CBD	2.4	2.5	2.6	2.5	2.9	2.5
	(0.01)	(0.01)	(0.01)	(0.02)	(0.02)	(0.03)
Mean	2.5	2.5	2.8	2.6	2.7	2.8

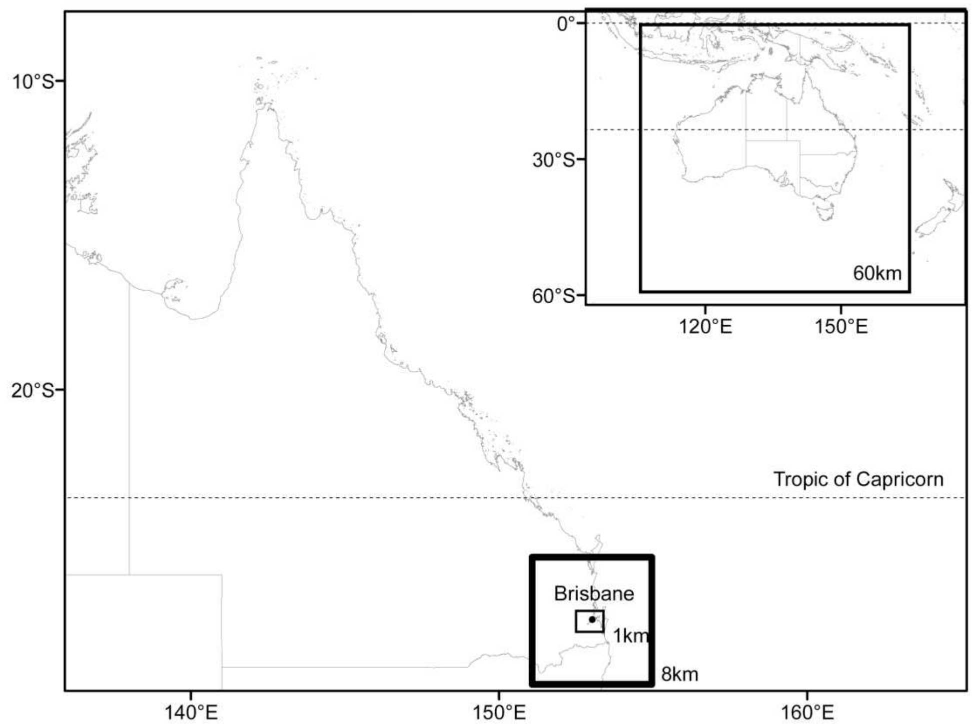

Figure 1. Location of study area, Brisbane, Australia and domain for 1 km and 8 km model resolution. Inset map: Domain for 60 km resolution. Dashed line shows Tropic of Capricorn.

210x156mm (300 x 300 DPI)

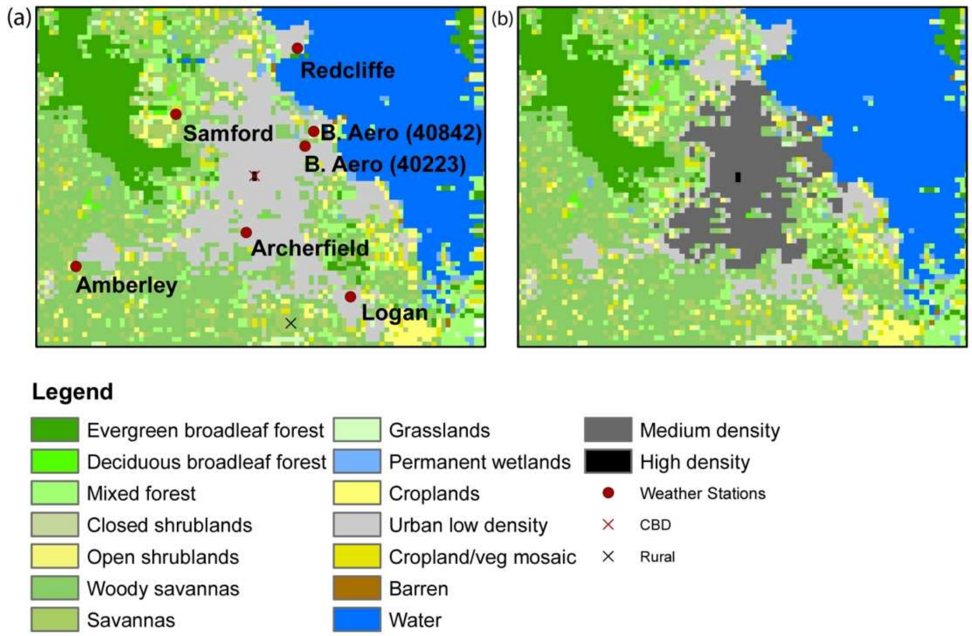

Figure 2. Land cover for Control (a) and Urban Growth (b) scenario. Red dots show locations of weather stations used in model validation. The two locations used to calculate the UHI are also shown (red cross = urban point used in UHI calculation, black cross = rural point used in UHI calculation).

170x112mm (300 x 300 DPI)

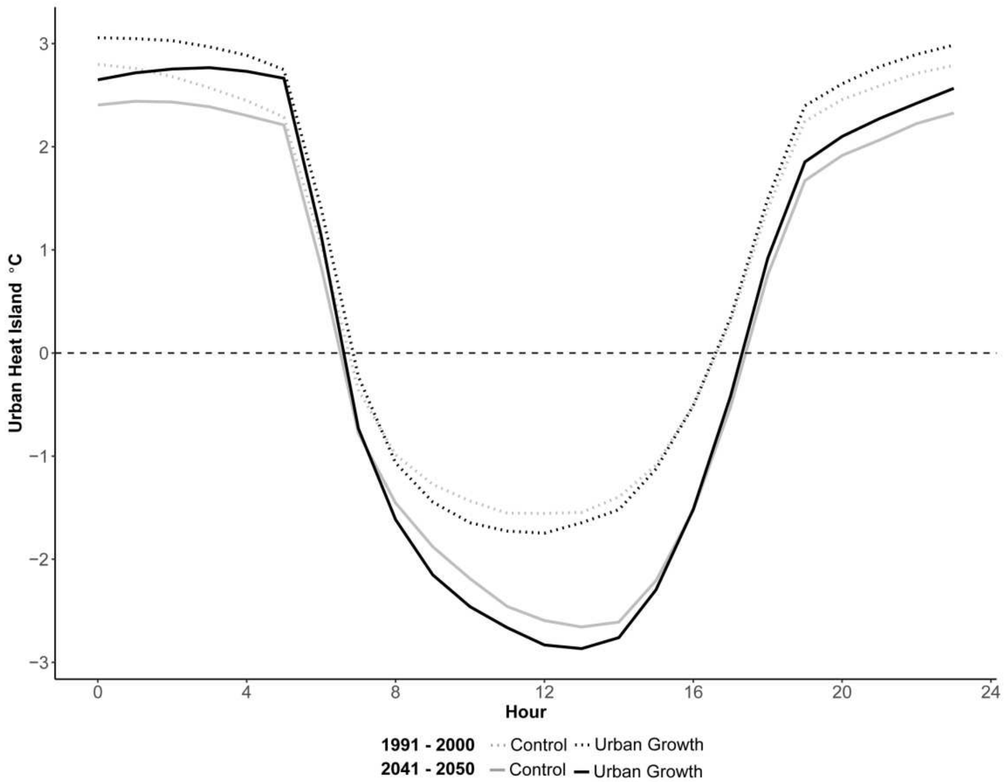

Figure 3. Hourly average summer (DJF) heat island for Control and Urban Growth scenario during 1991 – 2000 and 2041 – 2050.

240x196mm (300 x 300 DPI)

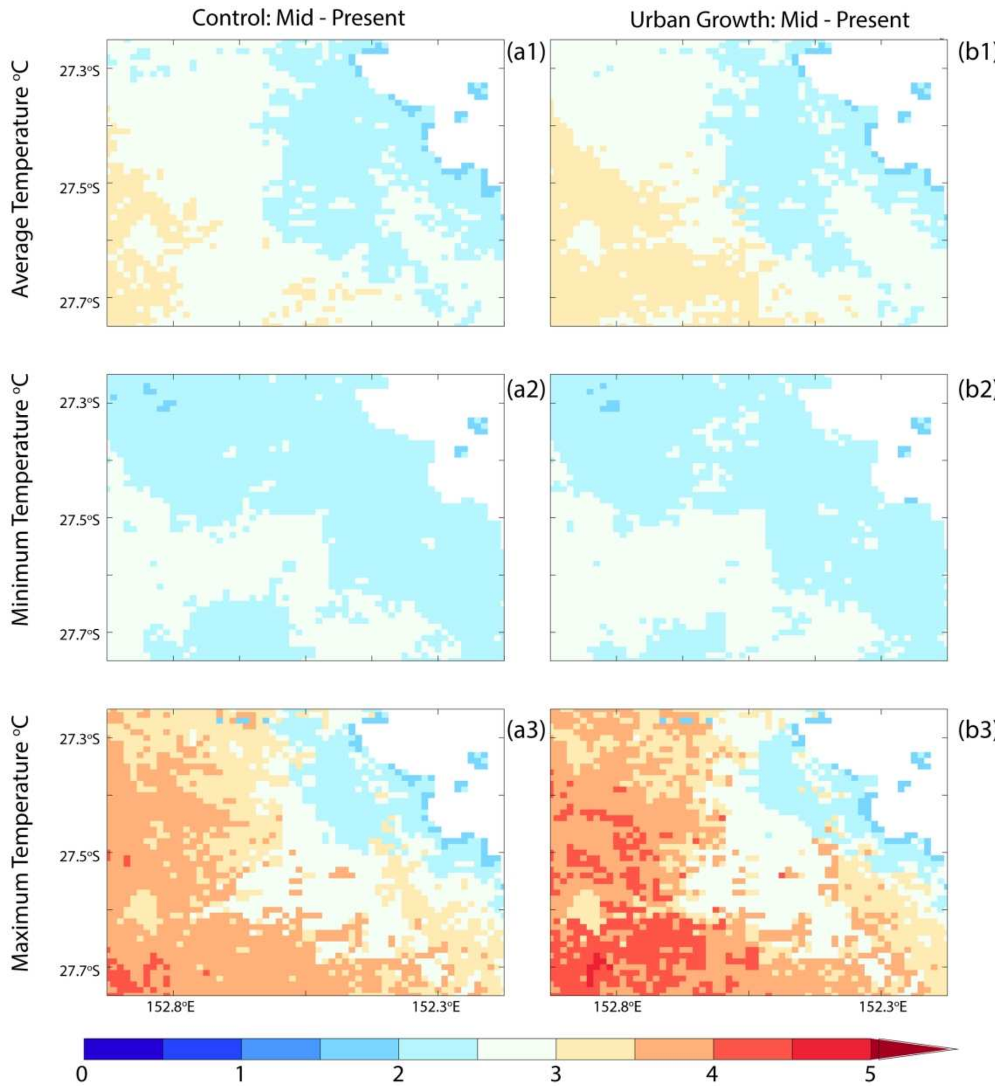

Figure 4. Change in average (row 1), minimum (row 2) and maximum (row 3) air temperature between the midterm (2041 – 2050) and present day (1991 – 2000) for the Control (column a) and Urban Growth (column b) scenario. Note, the Urban Growth scenario in the midterm is compared to the Urban Growth scenario in the present day, not to the Control scenario as in Table 4.

178x192mm (300 x 300 DPI)

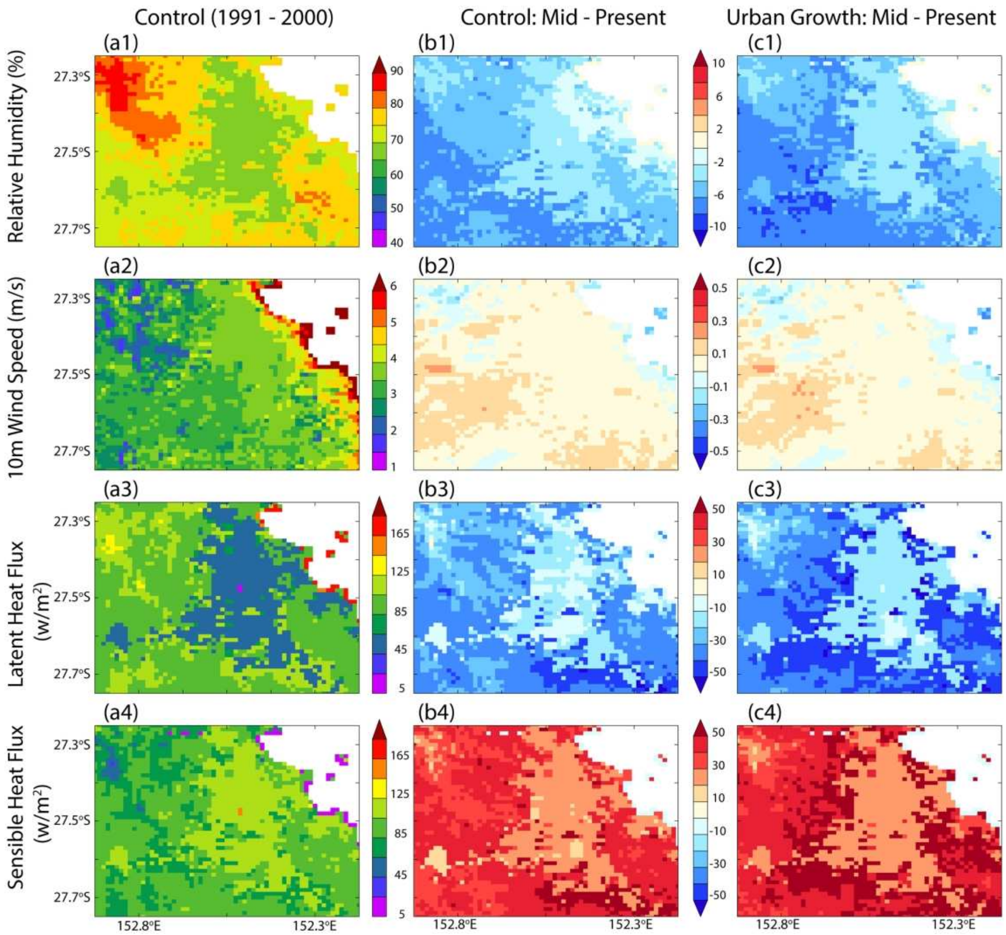

Figure 5. Change in relative humidity (row 1), 10m wind speed (row 2), latent and sensible heat flux (row 3 and 4) between the midterm and present day for the Control (column b) and Urban Growth (column c) scenario. Column a shows the present day values for the Control scenario. Column b is Control midterm – Control present day. Column c is Urban Growth midterm – Urban Growth present day.

169x156mm (300 x 300 DPI)

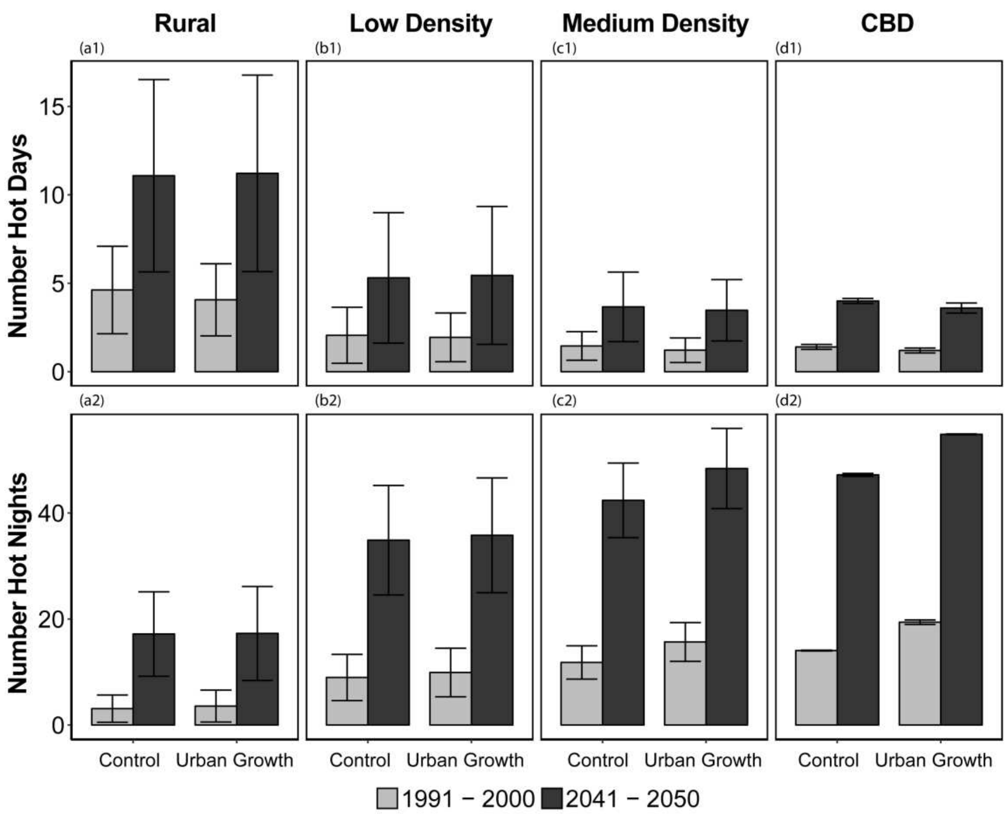

Figure 6. Average number of hot days and nights in summer (Dec – Feb) for rural and urban areas for Control and Urban Growth scenario. Only rural areas within the same elevation range as Brisbane city included in calculation of rural temperature change. Low Density areas refers to areas which were low density in both scenarios. Medium Density refers to areas which were medium density in the Urban Growth scenario, but low density in the Control scenario. Bars show spatial standard deviation. Hot days defined as day with maximum temperature above the 95th percentile of maximum temperature for 1991 – 2000 Control, rural areas. Hot nights defined same way, using minimum temperature. The threshold temperature for hot days was 40^0C, and 24^0C for hot nights. Note: The CBD covers a very small spatial area, which is why the error bars are small.

242x194mm (300 x 300 DPI)

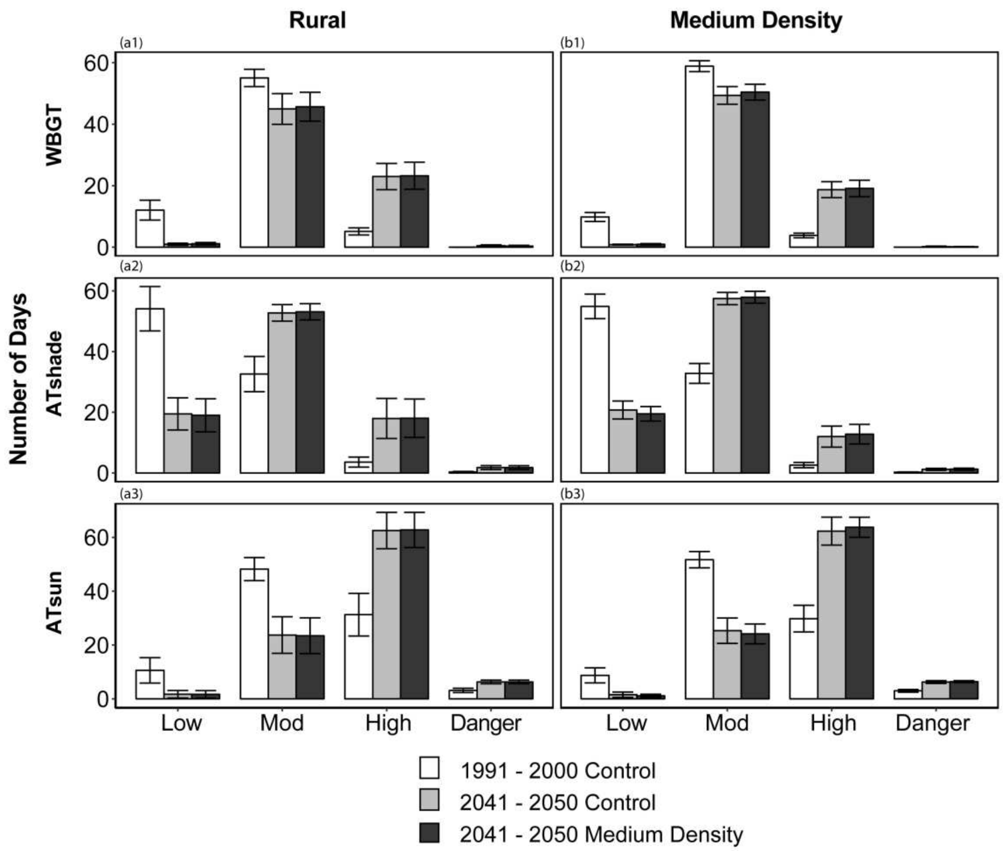

Figure 7: Average number of days per summer exceeding low, medium, high and dangerous thresholds of heat stress using WBGT (row 1), ATshade (row 2) and ATsun, (row 3) calculated using average temperature, for rural (column a) and CBD (column b) areas. Only rural areas within the same elevation range as Brisbane City were included in calculation of rural temperature change. Bars show spatial standard deviation.

245x210mm (300 x 300 DPI)